



Received: 27 December, 2024

Accepted: 17 January, 2025

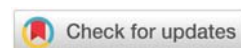
Published: 18 January, 2025

***Corresponding author:** Jin Sun Cha, Material Technology Center, Korea Testing Laboratory, Seoul, 08389, Republic of Korea, E-mail: jscha@ktl.re.kr

ORCID: <https://orcid.org/0000-0003-3350-6051>

Keywords: Hydrochar; Pyrochar; Lignin char; Cellulose char; Cadmium removal

Copyright License: © 2025 Cha JS, et al. This is an open-access article distributed under the terms of the Creative Commons Attribution License, which permits unrestricted use, distribution, and reproduction in any medium, provided the original author and source are credited.

<https://www.chemisgroup.us>


Research Article

Comparison of Hydrodchar and Pyrochar made from Cellulose, Lignin, and Cornhusk: Physiochemical Properties and removal of Cd(II) from Aqueous Solution

Jin Sun Cha^{1*}, Hyungjoo Kim² and Tae-Woo Kim³

¹Material Technology Center, Korea Testing Laboratory, Seoul, 08389, Republic of Korea

²Environmental New Business Center, Korea Testing Laboratory, Seoul, 08389, Republic of Korea

³Agency for Defense Development, Institute of Civil-Military Technology Cooperation, Daejeon, 34068, Republic of Korea

Abstract

In this study, hydrochar and pyrochar were made from cellulose, lignin (components of biomass), and corn husk (a type of biomass) through hydrothermal carbonization at 300 °C and pyrolysis at 300 °C and 500 °C. Their physiochemical properties and Cd(II) adsorption performances were then compared. Additionally, characteristics of hydrochar and pyrochar generated by each process were analyzed, including char generation yield, proximate & ultimate analysis, specific surface area (BET surface area) & porosity analysis, SEM & EDS (Scanning Electron Microscope & Energy Dispersive Spectrometer), FT-IR, pH_{pzc}, and so on. The pyrochar generated at the same temperature (300 °C) had higher char generation yield, ash content, and oxygen content with more oxygen functional groups than hydrochar. However, pyrochar had a lower specific surface area and pore volume than hypercar. By type of biomass, lignin showed the highest char generation yield. Regarding pH_{pzc}, corn husk had the highest value, followed by lignin and cellulose. Cd(II) adsorption characteristics in hydrochar and pyrochar were more suitable for the Langmuir adsorption model. It was found that the Cd(II) adsorption amount (116.8 mg/g) was the highest in PC-CH-500, which had high pH_{pzc} and inorganic content. As a result, electrostatic adsorption and cation exchange were the main mechanisms of Cd(II) adsorption under the condition of pH solution < pH_{pzc}.

Introduction

Biomass refers to renewable organic material that comes from lignocellulosic materials derived from living or living organic materials such as plants, animals, and agricultural residues [1,2]. Biomass, especially plant biomass, consists of lignin, cellulose, and hemicellulose [3]. The ratio of each component varies depending on the type of biomass. These components are strongly intermeshing, chemically bonded by non-covalent force, or cross-linked with each other. They have different characteristics depending on their connectivity and crystallinity [2,4]. In addition, since each component has a different decomposition temperature (for example,

hemicellulose has a decomposition temperature of 220–315 °C and lignin has a decomposition temperature of 160–900 °C), the biochar formation pathway and mechanism are different [4].

Biochar is known as a porous carbonaceous material produced by thermally decomposing biomass under little or no oxygen conditions [5]. Biochar has been the subject of many studies as an eco-friendly adsorbent for removing heavy metals due to its characteristics such as high carbon content, large surface parts, developed porous structures, surface functional groups, and inorganic compounds [6]. The thermal decomposition process in which biochar is produced can be classified into pyrolysis,

hydrothermal carbonization (HTC), torrefaction, and so on depending on the application temperature and holding time [3,5]. Pyrolysis refers to the process of thermally decomposing biomass in the temperature range of 300–900 °C under an inert atmosphere [6,7]. There are different ways of carrying out the pyrolytic process affecting the production of bio-oil, syngas, and carbonaceous residues (biochar). Especially, carbonization, the most ancient and known pyrolysis process, occurs at temperatures between 300 and 500 °C [1]. HTC process is a process of thermally decomposing biomass at 180–350 °C under oxygen-free, high-pressure (2–10 MPa) conditions in which subcritical water exists [8–10]. Due to different process characteristics, it has been reported that pyrochar generated char in pyrolysis and hydrochar generated in the HTC process have different characteristics. Sun, et al. [11] have studied the effects of feedstock type, production method, and temperature on pyrochar and hydrochar and reported that hydrochar has a higher acidic pH value and a lower carbon content than pyrochar. Fuertes, et al. [12] have produced carbonaceous products from corn stover by pyrolysis and hydrothermal carbonization and comparatively analyzed their characteristics. They reported that hydrochar has lower ash content and pH but a higher C recovery rate than pyrochar. Cao, et al. [13] compared chemical structures after generating hydrochar and slow-pyrolysis pyrochar with Swine-Manure. However, all these studies compared the properties of pyrochar and hydrochar produced at different temperatures.

Recent studies have compared adsorption characteristics in addition to the physicochemical properties of hydrochar and pyrochar. Wang, et al. [14] have produced hydrochar and pyrochar from Napier grass by hydrothermal carbonization (200 and 240 °C) and pyrolysis (300 and 500 °C) and conducted adsorption studies for Cd²⁺ sorption performances. They reported that the pyrochar had higher pH and ash content as well as better stability, while the hydrochar showed more oxygen functional groups. Researchers have explained that the pseudo-second-order kinetic model best fitted the Cd²⁺ sorption kinetics of biochars, the pyrochar exhibited better Cd²⁺ sorption capacity. Huff, et al. [15] have produced pinewood, peanut shell, and bamboo biochar by hydrothermal conversion and pyrolysis and conducted a comparative study on methylene blue adsorption properties. They reported that HTC was higher in CEC (Cation Exchange Capacity) than biochar due to a higher oxygen functional group and O: C ratio. However, the adsorption performance of methylene blue was not proportional to CEC. Elaigwu, et al. [16] have produced *Prosopis africana* (a flowering plant) shell char by pyrolysis and hydrothermal carbonization and studied Pb²⁺ and Cd²⁺ removal performance. They reported that the performance of hydrochar for Pb and Cd removal was higher than that of biochar. However, Babeker, et al. [17] reported that the Cu adsorption capacity of pyrochar derived from Acacia Senegal waste was seven times that of hydrochar. These studies compared the characteristics and adsorption capacity of hydrochar and biochar produced at different temperatures.

Therefore, in this study, pyrochar and hydrochar were produced from cellulose, lignin (which are components

of biomass), and corn husk (a type of biomass) at the same temperature (300 °C). Additionally, pyrochar was generated at a general pyrolysis temperature (500 °C). Cellulose is the most abundant organic compound that can be found in nature possessing a structural function in plant cell walls [18] Lignin is also contained in plant cell walls, which plays a role in binding, cementing, and putting the fibers together [1]. In this study, physicochemical characteristics according to the biochar generation process for each biomass component were then compared. Adsorption performances of biochar for Cd(II), which is a highly persistent environmental toxicant and inflicts chronic intoxication by directly destroying the creatural urinary system [19], were compared by using two different isotherm models. This study will provide valuable insights into the potential Cd mechanism and water pollution prevention strategies by elucidating the differences in properties of biochar produced from biomass components (lignin, cellulose) and biochar produced from corn husk, which are composed of these materials.

Material and methods

Biochar preparation

To generate pyrochar (PC) through pyrolysis, each cellulose (C), lignin (L), and corn husk (CH) was put into a pyrolysis device. After that, while N₂ was injected, the temperature was raised from room temperature to 300 °C (or 500 °C) at 10 °C/min and maintained at the corresponding temperature for 1 hour. The pyrochar generated in this way was named PC-C-x, PC-L-x, or PC-CH-x (x = 300 or 500). Hydrochar using hydrocarbonization was prepared by mixing biomass with H₂O at 1: 5 weight ratio, which was then put into a Parr reactor (Model 4545, Parr Instrument Co.) and reacted at 300 °C for 1 hour. After the reaction, the mixture of water and hydrochar (HC) was separated through filtration. Hydrochar was dried at 100 °C in an oven for 24 hours. Hydrochar generated from this process was expressed as HC-C-300, HC-L-300, or HC-CH-300.

Biochar characterization

The ultimate analysis to determine the contents of C, H, N, and S for each raw biomass and generated biochar was analyzed using an elemental analyzer (Flash 200, Thermo). O content was calculated as the remaining content. Moisture, volatile, ash, and fixed carbon contents were analyzed using a thermogravimetric analyzer (TGA701, LECO). Proximate analysis was carried out to obtain the values of Moisture, volatile, ash, and fixed carbon contents using a thermogravimetric analyzer (TGA701, LECO). The specific surface area and porosity of each sample were analyzed using the N₂ adsorption-desorption method (3Flex, Micromeritics) that could analyze the BET surface area, pore volume, and pore size. Surface characteristics and chemical compositions of char generated according to the application process and temperature were analyzed using FE-SEM (Field Emission-Scanning Electron Microscopy, MIRA 3 XMU, TESCAN) and EDS (Energy Dispersive Spectrometer, X-act, OXFORD). Functional groups on the sample surface were analyzed by FT-IR (Fourier transform infrared spectroscopy,

Nicolet 6700, Thermo) with a wavenumber range of 4000–400 cm^{-1} and a resolution of 4 cm^{-1} . pH values at the point of zero charges (pH_{pzc}) were measured according to previous studies [20,21]. After adding 0.1 M NaOH and 0.1 M HCl to 10 ml of 0.01 M NaCl to adjust the pH from 2 to 9 ($\text{pH}_{\text{initial}}$), 30 mg of biochar was added to the NaCl solution adjusted to each pH followed by shaking at 300 rpm for 48 hours. After measuring the final pH (pH_{final}), the final pH subtracted from the initial pH was defined as ΔpH ($\Delta\text{pH} = \text{pH}_{\text{final}} - \text{pH}_{\text{initial}}$). pH_{pzc} was determined as the pH when $\Delta\text{pH} = 0$ in the ΔpH vs. $\text{pH}_{\text{initial}}$ profile.

Adsorption experiment

Each char was added to the Cd(II) aqueous solution and reacted to examine the Cd(II) adsorption performance. The adsorption efficiency was evaluated by measuring the concentration of Cd(II) before and after the reaction. An aqueous solution of Cd(II) at a concentration of 50 mg/L was prepared with $\text{CdCl}_2 \cdot 2\frac{1}{2}\text{H}_2\text{O}$ (Sigma Aldrich Chemical Co.). The pH of the aqueous solution was 6.0. Each char of 0.05 g was added to 20 mL of the aqueous solution of Cd(II) at each concentration and shaken at a speed of 250 rpm for 18 hours at room temperature. After the reaction, filtration was performed using a qualitative filter paper (Adventec, 0.45 μm). The concentration of Cd(II) was measured using ICP-OES (Inductively Coupled Plasma – Optical Emission Spectrometry, OPTIMA 8300, Perkin Elmer). The isothermal adsorption was evaluated based on adsorption performance with Results and discussion.

Characterization of hydrochars and pyrochars

Yield, proximate, and elemental analysis: Table 1 summarizes biochar production yield with ultimate and proximate analysis results of cellulose, lignin, corn husk, pyrochar, and hydrochar. The biochar yield was determined as the ratio of the mass of the biochar product to the mass of the biomass using the following equation (1) shown below:

$$\text{Yield (\%)} = \frac{\text{mass of biochar (g)}}{\text{mass of biomass (g)}} \times 100 \quad (1)$$

It was found that lignin had the highest yield, followed by

cellulose and corn husk. Muley, et al. [22] have reported that lignin is composed of a cross-linking macromolecule. Thus, lignin is a material constituting a cell wall of biomass. Muley, et al. [22] also reported that lignin was relatively thermally stable with a complex molecular structure and had a high char yield due to its high fixed carbon content, while cellulose had relatively low thermal stability and fixed carbon content [22]. Corn husk as a biomass containing hemicellulose is decomposed at 180–350 $^{\circ}\text{C}$ [23]. Therefore, most hemicellulose composing corn husk was decomposed and the char yield was lower than that of cellulose at 300 $^{\circ}\text{C}$. However, at 500 $^{\circ}\text{C}$, the char yield was higher than that of cellulose under the influence of thermally stable lignin. When the thermal decomposition temperature was the same, the yield of HC was lower than that of PC. Kambo, et al. [2] have explained that in a hydrothermal condition, some biomass polymers are converted into an aqueous phase due to subcritical water, leading to decreased solid product.

When their thermal decomposition temperatures are the same, the oxygen content of pyrochar is higher than that of hydrochar. In the case of pyrochar, as the thermal decomposition temperature increased, the C content increased while the O and H contents decreased. According to the Van Krevelen diagram, raw biomass has high O/C and H/C, while O/C and H/C are very low after slow pyrolysis. HC is similar to slow pyrolysis and O/C, whereas H/C is high [24]. Figure 1 shows the O/C vs. H/C of pyrochar and hydrochar. In the case of lignin, O/C and H/C were somewhat low due to its high C content. When the thermal decomposition temperature was 300 $^{\circ}\text{C}$, O/C and H/C of PC were similar to HC. However, as the pyrolysis temperature increased by 500 $^{\circ}\text{C}$, O/C and H/C decreased, resulting in similar results to Van Krevelen's diagram overall. High H/C and O/C in HC-300 and PC-300 meant low carbonization of biomass, indicating that high contents of non-carbonizable organic matter were present in biochar [25].

As a result of the ultimate analysis, when the thermal decomposition temperature was the same, the C content of cellulose having a low decomposition temperature was found to be higher than that of lignin and the fixed carbon content

Table 1: Physico-chemical properties and yield of raw biomass (cellulose, lignin, corn husk), HC-C-300 (cellulose hydrochar at 300 $^{\circ}\text{C}$), HC-L-300 (lignin hydrochar at 300 $^{\circ}\text{C}$), HC-CH-300 (corn husk hydrochar at 300 $^{\circ}\text{C}$), PC-C-300 (cellulose pyrochar at 300 $^{\circ}\text{C}$), PC-L-300 (lignin pyrochar at 300 $^{\circ}\text{C}$), PC-CH-300 (corn husk pyrochar at 300 $^{\circ}\text{C}$), PC-C-500 (cellulose pyrochar at 500 $^{\circ}\text{C}$), PC-L-500 (lignin pyrochar at 500 $^{\circ}\text{C}$), PC-CH-500 (corn husk pyrochar at 500 $^{\circ}\text{C}$).

	Ultimate analysis					Proximate analysis				Composition analysis							yield (%)
	C	H	O ^a	N	S	moisture	Volatile mass	Fixed carbon	Ash	C	O	S	K	Si	Na	Mg	
Cellulose	41.98	6.34	51.66	0.02	0.00	-	-	-	-	-	-	-	-	-	-	-	-
Lignin	61.73	5.61	31.51	0.68	0.47	4.21	62.05	32.25	1.49	-	-	-	-	-	-	-	-
Corn Husk	44.00	5.83	49.51	0.66	0.00	7.39	75.55	14.22	2.85	-	-	-	-	-	-	-	-
HC-C-300	82.37	3.92	13.63	0.09	0.00	1.86	47.06	50.89	0.19	88.39	10.94	0.67	-	-	-	-	43.3
HC-L-300	71.30	4.93	22.98	0.46	0.33	1.69	50.98	45.45	1.89	72.47	25.45	2.07	-	-	-	-	70.9
HC-CH-300	75.03	4.91	18.91	1.16	0.00	1.91	50.91	44.80	2.40	73.74	25.32	0.86	-	0.13	-	-	37.2
PC-C-300	72.62	4.33	22.95	0.11	0.00	3.18	58.58	37.48	0.77	75.52	23.66	0.83	-	-	-	-	45.5
PC-L-300	70.56	4.68	23.31	0.76	0.69	1.10	52.77	44.08	2.06	69.13	27.36	2.34	-	-	1.18	-	72.7
PC-CH-300	63.96	4.45	30.36	1.23	0.00	2.65	54.11	36.96	6.27	65.35	31.04	0.98	1.74	0.66	-	0.23	40.8
PC-C-500	88.72	2.83	8.30	0.16	0.00	1.32	23.34	75.04	0.80	88.79	10.47	0.75	-	-	-	-	23.8
PC-L-500	82.41	2.56	13.58	0.86	0.58	2.14	34.33	58.73	4.80	83.99	10.45	3.56	0.45	-	1.57	-	58.2
PC-CH-500	77.17	1.38	18.96	1.38	0.00	2.95	26.02	61.02	10.02	62.97	24.27	3.60	5.11	6.12	-	0.57	25.6

^a difference

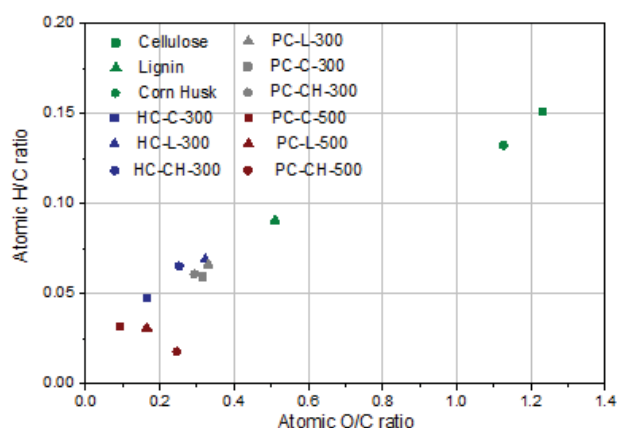


Figure 1: Atomic H/C ratios and O/C ratio of of raw biomass(cellulose, lignin, corn husk), HC-C-300(cellulose hydrochar at 300 °C), HC-L-300(lignin hydrochar at 300 °C), HC-CH-300(corn husk hydrochar at 300 °C), PC-C-300(cellulose pyrochar at 300 °C), PC-L-300(lignin pyrochar at 300 °C), PC-CH-300(corn husk pyrochar at 300 °C), PC-C-500(cellulose pyrochar at 500 °C), PC-L-500(lignin pyrochar at 500 °C), PC-CH-500(corn husk pyrochar at 500 °C).

of hydrochar was higher than that of pyrochar. In the case of pyrochar, as the decomposition temperature increased, the fixed carbon and ash content increased as the yield and volatile content of char decreased due to the decomposition of non-carbonizable organic matter. In particular, when the temperature was the same, the ash content of pyrochar was found to be higher than that of hydrochar. F, et al. (2018) have explained that this is because it is dissolved in inorganic compounds by subcritical water in the process of hydrothermal carbonization of hydrochar generation. These results were also confirmed by component analysis using EDS. Alkaline and alkaline earth metals such as K, Na, and Mg were detected in pyrochar, while no corresponding components were detected in hydrochar. Thus, it seemed that they were dissolved in water during the production process.

Specific surface area and porosity: Table 2 summarizes the specific surface area and porosity of char generated by biomass type and char reaction conditions. When thermal decomposition temperatures were the same, it was found that the specific surface area and pore volume were in the order of corn husk > cellulose > lignin. A low specific surface area means an underdeveloped porous structure and an incomplete carbonization [26]. The specific surface area and pores were developed in corn husk because hemicellulose was decomposed and pores were formed, whereas in lignin known to be relatively thermally stable, specific surface area and pores were not developed. As increasing the pyrolysis temperature, more specific surface area and pore volume were developed. Kambo, et al. [2] have explained that void formed in biochar due to volatilization of organic compounds can result in the development of specific surface area and pore volume.

Surface characterization: Figure 2 shows the results of surface characteristics of hydrochars and pyrochars produced according to the type of biomass and char reaction conditions. Different shapes appeared depending on the type of raw material. Cellulose was found that the circular shape of short fiber was maintained even after the thermal decomposition

process, whereas lignin had a shape in which the surface was cut after the thermal decomposition reaction.

Biochar produced at the same temperature in different thermal processes was verified that more pores were formed in a hydrochar than in a pyrochar. More pores were developed as temperature increased in the pyrochars. This trend was the same as the analysis results of specific surface area and pore characteristics. At the same temperature, specific surface area and pore volume were higher in hydrochar than in pyrochar. For pyrochar prepared at a higher temperature, a larger specific surface area and pore were also found based on shape measurements in Figure 2.

Figure 3 shows FT-IR analysis results of hydrochars and pyrochars generated according to the type of biomass and reaction conditions. Also, Table 3 summarizes function groups by wavenumber [19,26]. The functional groups of cellulose and corn husk char produced at 300 °C were similar. However, lignin had slightly different results. Similar results have been

Table 2: Specific surface areas and porosities of HC-C-300(cellulose hydrochar at 300 °C), HC-L-300(lignin hydrochar at 300 °C), HC-CH-300(corn husk hydrochar at 300 °C), PC-C-300(cellulose pyrochar at 300 °C), PC-L-300(lignin pyrochar at 300 °C), PC-CH-300(corn husk pyrochar at 300 °C), PC-C-500(cellulose pyrochar at 500 °C), PC-L-500(lignin pyrochar at 500 °C), PC-CH-500(corn husk pyrochar at 500 °C).

	BET Surface area(m ² /g)	Total Pore Volume(cm ³ /g)	Pore Size(nm)
HC-C-300	4.47	0.0017	0.95
HC-L-300	0.41	0.0001	0.71
HC-CH-300	1.43	0.0038	1.44
PC-C-300	0.83	0.0003	1.36
PC-L-300	0.07	0.0000	0.89
PC-CH-300	0.39	0.0003	1.68
PC-C-500	462.87	0.2018	1.74
PC-L-500	86.62	0.0470	2.17
PC-CH-500	78.65	0.0377	1.92

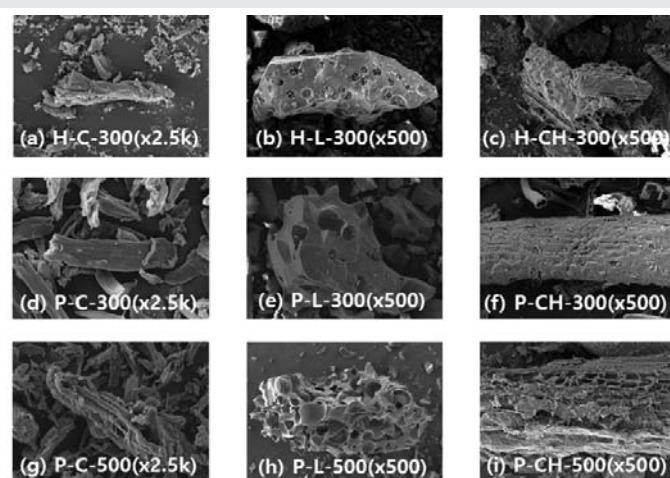


Figure 2: Scanning Electron Microscope (SEM) images of of HC-C-300(cellulose hydrochar at 300 °C), HC-L-300(lignin hydrochar at 300 °C), HC-CH-300(corn husk hydrochar at 300 °C), PC-C-300(cellulose pyrochar at 300 °C), PC-L-300(lignin pyrochar at 300 °C), PC-CH-300(corn husk pyrochar at 300 °C), PC-C-500(cellulose pyrochar at 500 °C), PC-L-500(lignin pyrochar at 500 °C), PC-CH-500(corn husk pyrochar at 500 °C).

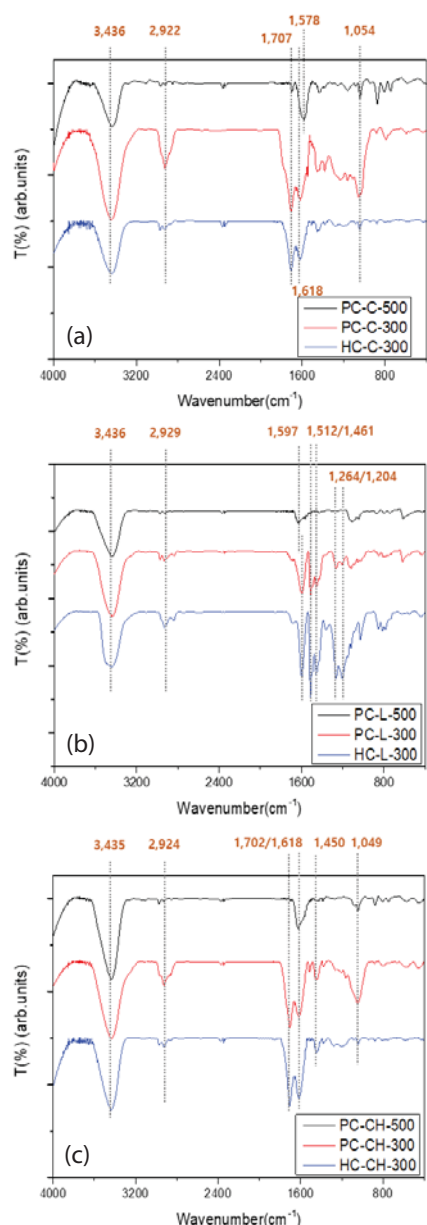


Figure 3: FT-IR spectra of HC-C-300(cellulose hydrochar at 300 °C), HC-L-300(lignin hydrochar at 300 °C), HC-CH-300(corn husk hydrochar at 300 °C), PC-C-300(cellulose pyrochar at 300 °C), PC-L-300(lignin pyrochar at 300 °C), PC-CH-300(corn husk pyrochar at 300 °C), PC-C-500(cellulose pyrochar at 500 °C), PC-L-500(lignin pyrochar at 500 °C), PC-CH-500(corn husk pyrochar at 500 °C).

reported previously [27]. Researchers have explained that the characteristics of lignin in the biochar generated in moderate temperatures are not dominant. Unlike cellulose char or corn husk char, in HC-L-300 and PC-L-300, bands were formed at 1204 cm⁻¹, 1264 cm⁻¹, and so on. The band at 1204 cm⁻¹ was due to C-O stretching vibration and the band at 1264 cm⁻¹ was due to C=C aromatic ring vibration as summarized in Table 3. The formation of these bands means that the C=C and C-O bonds of lignin are not completely decomposed [19]. The band's size decreased as the pyrolysis increased from 300 °C to 500 °C because carbonization occurred as the temperature increased [26]. It was found that bands at about 1050 cm⁻¹ and 2920 cm⁻¹ were large in PC-C-300 and PC-CH-300, while their sizes were relatively small in HC, PC-C500, and PC-CH-500.

This was because C-O and aliphatic C-H were not completely decomposed in PC-300 while C-O and C-H bonds were broken at a high temperature or hydrothermal carbonization. In particular, the formation of 1578 cm⁻¹ band after 2922 cm⁻¹ band reduction due to an increase in pyrolysis temperature was due to the decomposition of aliphatic carbon of cellulose to form aromatic carbon [28]. It seems that pyrolysis is advantageous for the formation of functional groups while hydrothermal carbonization is advantageous for surface area and pore formation when thermal decomposition at a moderate temperature.

Adsorption experiments

Adsorption isotherm experiments can be used to investigate the mechanism for the interaction between the adsorbent and the adsorbate. To investigate the adsorption characteristics of Cd(II) by pyrochar and hydrochar, the amount of adsorbent was fixed at 0.05 g. Isothermal adsorption characteristics were then evaluated according to the concentration of the adsorption (Cd(II)). Two adsorption isotherm models used frequently are the Langmuir and Freundlich models. The Langmuir model is an adsorption formula applied under the assumption that the adsorbent is adsorbed into a monomolecular layer on the surface of the adsorbent. It is expressed with Equation (2) shown below:

$$q_e = \frac{q_m K_L C_e}{1 + K_L C_e} \quad (2)$$

If this is expressed in a linear equation, it can be expressed as Equation (3) shown below:

$$\frac{1}{q_e} = \frac{1}{K_L \times q_m} \frac{1}{C_e} + \frac{1}{q_m} \quad (3)$$

Where C_e is the equilibrium concentration of Cd(II) in solution(mg/L), q_m is the maximum adsorbed amount per unit mass of adsorbent (mg/g), and K_L is the Langmuir constant. Results are summarized in Table 4.

The Freundlich model represents the relationship between

Table 3: Functional groups of Fourier-Transform Infrared Spectroscopy (FT-IR) spectra of HC-C-300(cellulose hydrochar at 300 °C), HC-L-300(lignin hydrochar at 300 °C), HC-CH-300(corn husk hydrochar at 300 °C), PC-C-300(cellulose pyrochar at 300 °C), PC-L-300(lignin pyrochar at 300 °C), PC-CH-300(corn husk pyrochar at 300 °C), PC-C-500(cellulose pyrochar at 500 °C), PC-L-500(lignin pyrochar at 500 °C), PC-CH-500(corn husk pyrochar at 500 °C).

Wavenumber(cm ⁻¹)	Functional group	Description
3435~6	O-H stretching	Hydroxyl or carboxyl groups
2922~9	C-H stretching	Aliphatic
about 1700	C=O stretching	Carbonyl, ester, or carboxyl
1510-1600	C=C stretching	Aromatic skeletal in lignin
1420-1460	C-H deformation C=C stretching C=O stretching	C-H deformation carbohydrates aromatic and carboxylic compounds from carboxylic compounds
1100-1260	C-O stretching	Aromatic of methoxyl and phenyl propane structure
1050-1060	C-O stretching	-

the amount of adsorbent adsorbed to the adsorbent and the concentration of solution. It is defined as $q_e = K_F C_e^{1/n}$. By taking logs on both sides, it can be expressed as equation (4) shown below:

$$\ln q_e = \ln K_F + \frac{1}{n} \ln C_e \quad (4)$$

Where q_e is the amount of Cd(II) adsorbed per unit weight of the adsorbent (mg/g), K_F and n are Freundlich constants, and C_e is the equilibrium concentration (mg/L) of Cd(II) in the solution. The linear plot of the Langmuir and Freundlich adsorption isotherm of Cd(II) is shown in Figure 4 and the results of the Freundlich isotherm are summarized in Table 4. The q_m , K_L , and R^2 values of the Langmuir model were obtained by plotting $1/q_e$ vs. $1/C_e$ (Figure 4(a)). Also, K_F , $1/n$, and R^2 values of the Freundlich model were obtained by plotting $\ln(q_e)$ vs. $\ln(C_e)$ (Figure 4(b)).

Results showed that adsorption characteristics of Cd(II) by pyrochar and hydrochar in the Langmuir model were more suitable than those in the Freundlich model, with an R^2 of 0.99 or higher. The Cd(II) was adsorbed as a monomolecular layer on the surface of the pyrochar and hydrochar. Yan, et al. [29] reported the adsorption isotherm of Pb and Cd on corn stalk biochar can be well described by the Langmuir model, Sangsuk, et al. [30] also reported that the adsorption of methylene blue on the BP(*Biden pilosa*) biochar followed the Langmuir adsorption isotherm, that was similar results as in this study.

Comparing adsorption results with cellulose char, the PC-C-500 had a specific surface more than 100 times larger than that of HC-C-300, whereas the adsorption amount was lower than that of HC-C-300. Zama, et al. [31] have reported that physical characteristics such as specific surface area of biochar have little effect on heavy metal removal in a study on the effect of physicochemical properties of biochar produced at different temperatures on the absorption and desorption of heavy metals (Pb, Cd, As). Figure 5 summarizes pH_{pzc} (point of zero charge) measurement results for each type of pyrochar and hydrochar. pH_{pzc} refers to the pH value in which the sum of the surface positive charges is balanced with the sum of the surface negative charges. The surface of the adsorbent has a positive charge at

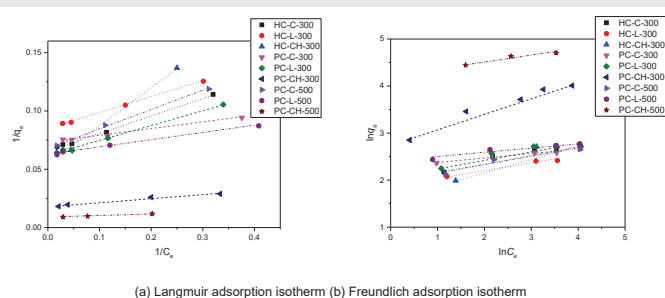


Figure 4: Linear plot of the Cd(II) adsorption following the Langmuir and Freundlich model by HC-C-300(cellulose hydrochar at 300 °C), HC-L-300(lignin hydrochar at 300 °C), HC-CH-300(corn husk hydrochar at 300 °C), PC-C-300(cellulose pyrochar at 300 °C), PC-L-300(lignin pyrochar at 300 °C), PC-CH-300(corn husk pyrochar at 300 °C), PC-C-500(cellulose pyrochar at 500 °C), PC-L-500(lignin pyrochar at 500 °C), PC-CH-500(corn husk pyrochar at 500 °C).

a pH below pH_{pzc} , but has a negative charge at a pH higher than pH_{pzc} [32]. Tran, et al. [33] have applied the pH_{pzc} ΔpH calculation formula ($\Delta pH = pH_{initial} - pH_{final}$) for pH_{pzc} in a relevant study as opposed to this study ($\Delta pH = pH_{final} - pH_{initial}$). According to their study results, by changing the formula applied in this study, in the case of $pH_{solution} > pH_{pzc}$, the surface of biochar had a positive charge by protonation of acid groups. Metal sorption is inhibited because of an electrostatic repulsion between Cd(II) ions and functional groups, so the adsorption amount was measured to be low [32]. Researchers have explained that in the case of $pH_{solution} > pH_{pzc}$, complexation or surface precipitation is the primary mechanism of heavy metal removal. Through FT-IR results, many functional groups such as -OH, C-O, and C=O were formed in PC-C-300. It was judged that Cd(II) was removed through surface complexation by oxygen functional groups. Han, et al. [34] have also announced that the lower Sb(III) and Cd(II) adsorption performance in hydrochar than pyrochar due to low contents of surface functional groups and fewer negative charges, consistent with the results of this study. Cd(II) adsorption amount of lignin pyrochar (PC-L-300, 500) was slightly higher than that of cellulose pyrochar pyrochar (PC-C-300, 500), while the adsorption amount of cellulose hydrochar (HC-C-300) was higher than that of lignin hydrochar (HC-L-300). As a result of EDS analysis, inorganic substances such as Na and K were not detected in HC-L-300, whereas Na contents were measured to be 1.18% and 1.57% in PC-L-300 and PC-L-500, respectively. Na contents were decreased to 0.93% and 1.19% after adsorption by PC-L-300 and PC-L-500, respectively. Deng, et al. [35] have explained that K, Ca, Na, Mg, and so on of biochar can be exchanged with ions such as Cd during the adsorption process. The amount of Cd(II) adsorption increased due to cation exchange between Na and Cd. In addition, the Na content was higher in PC-L-500 than in PC-L-300, although the adsorption amount was measured to be slightly higher in PC-L-300, which was considered to be due to the effect of surface complexation by oxygen function groups formed in PC-L-300.

Corn husk char had a higher Cd(II) adsorption than cellulose or lignin char. In particular, the adsorption amount increased significantly in PC-CH-300 and PC-CH-500. As shown in Figure 5, pH_{pzc} values of PC-CH-300 and PC-CH-500 were about 7.5 and 8.8, respectively, meaning that the surface of char was negatively charged. Thus, Cd(II) was adsorbed onto the

Table 4: Results of isotherm model on adsorption of Cd(II) by HC-C-300(cellulose hydrochar at 300 °C), HC-L-300(lignin hydrochar at 300 °C), HC-CH-300(corn husk hydrochar at 300 °C), PC-C-300(cellulose pyrochar at 300 °C), PC-L-300(lignin pyrochar at 300 °C), PC-CH-300(corn husk pyrochar at 300 °C), PC-C-500(cellulose pyrochar at 500 °C), PC-L-500(lignin pyrochar at 500 °C), PC-CH-500(corn husk pyrochar at 500 °C).

	Langmuir model			Freundlich model		
	q_m (mg/g)	K_L	R^2	K_F	$1/n$	R^2
HC-C-300	15.17	0.441	0.9968	6.817	0.234	0.9569
HC-L-300	11.79	0.628	0.9991	6.672	0.153	0.9760
HC-CH-300	17.81	0.175	0.9933	5.086	0.302	0.9069
PC-C-300	13.71	1.298	0.9923	10.017	0.088	0.8660
PC-L-300	16.26	0.476	0.9966	8.458	0.167	0.8935
PC-CH-300	56.52	0.312	0.9965	16.495	0.331	0.9646
PC-C-500	14.65	0.417	0.9978	7.192	0.176	0.9388
PC-L-500	15.99	1.026	0.9939	10.813	0.102	0.9350
PC-CH-500	116.80	0.547	0.9993	70.046	0.135	0.9372

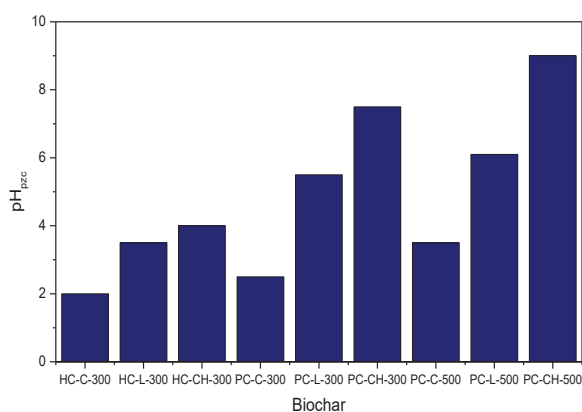


Figure 5: pH_{pzc} values of HC-C-300(cellulose hydrochar at 300 °C), HC-L-300(lignin hydrochar at 300 °C), HC-CH-300(corn husk hydrochar at 300 °C), PC-C-300(cellulose pyrochar at 300 °C), PC-L-300(lignin pyrochar at 300 °C), PC-CH-300(corn husk pyrochar at 300 °C), PC-C-500(cellulose pyrochar at 500 °C), PC-L-500(lignin pyrochar at 500 °C), PC-CH-500(corn husk pyrochar at 500 °C).

References

1. Tursi A. A review on biomass: importance, chemistry, classification, and conversion. *Biofuel Res J.* 2019;22:9662-979. Available from: <https://doi.org/10.18331/BRJ2019.6.2.3>
2. Kambo HS, Dutta A. A comparative review of biochar and hydrochar in terms of production, physico-chemical properties and applications. *Renew Sustain Energy Rev.* 2015;45:359–378. Available from: <https://doi.org/10.1016/j.rser.2015.01.050>
3. Rutherford DW, Wershaw RL, Rostad CE, Kelly CN. Effect of formation conditions on biochars: Compositional and structural properties of cellulose, lignin, and pine biochars. *Biomass Bioenergy.* 2012;46:693-701. Available from: <http://dx.doi.org/10.1016/j.biombioe.2012.06.026>
4. Li Y, Xing B, Ding Y, Han X, Wang S. A critical review of the production and advanced utilization of biochar via selective pyrolysis of lignocellulosic biomass. *Bioresour Technol.* 2020;312:123614. Available from: <https://doi.org/10.1016/j.biortech.2020.123614>
5. Xiang W, Zhang X, Chen J, Zou W, He F, Hu X, Tsang DCW, Ok YS, Gao B. Biochar technology in wastewater treatment: A critical review. *Chemosphere.* 2020;252:126539. Available from: <https://doi.org/10.1016/j.chemosphere.2020.126539>
6. Xiao R, Awasthi MK, Li RH, Park JH, Pensky SM, Wang Q, et al. Recent developments in biochar utilization as an additive in organic solid waste composting: A review. *Bioresour Technol.* 2017;246:203-213. Available from: <https://doi.org/10.1016/j.biortech.2017.07.090>
7. Cha JS, Park SH, Jung SH, Ryu CK, Jeon JK, Shin MC, et al. Production and utilization of biochar: A review. *J Ind Eng Chem.* 2016;40:1-5. Available from: <https://www.scrip.org/reference/referencespapers?referenceid=1970283>
8. Lin Y, Ma X, Peng X, Hu S, Yu Z, Fang S. Effect of hydrothermal carbonization temperature on combustion behavior of hydrochar fuel from paper sludge. *Appl Therm Eng.* 2015;91:574-582. Available from: <https://doi.org/10.1016/j.applthermaleng.2015.08.064>
9. He C, Giannis A, Wang JY. Conversion of sewage sludge to clean solid fuel using hydrothermal carbonization: Hydrochar fuel characteristics and combustion behavior. *Appl Energy.* 2013;111:257-266. Available from: <https://doi.org/10.1016/j.apenergy.2013.04.084>
10. Mumme J, Eckervogt L, Pielert J, Diakite M, Rupp F, Kern J. Hydrothermal carbonization of anaerobic digested maize silage. *Bioresour Technol.* 2011;102:9255-9260. Available from: <https://doi.org/10.1016/j.biortech.2011.06.099>
11. Sun Y, Gao B, Yao Y, Fang J, Zhang M, Zhou Y, et al. Effects of feedstock type, production method, and pyrolysis temperature on biochar and hydrochar properties. *Chem Eng J.* 2014;240:574-578. Available from: <https://www.scrip.org/reference/referencespapers?referenceid=3095434>
12. Fuertes AB, Arbustain MC, Sevillas M, Macia-Agullo MJ, Fiol S, Lopez R, et al. Chemical and structural properties of carbonaceous products obtained by pyrolysis and hydrothermal carbonization of corn stover. *Aust J Soil Res.* 2010;48:618-626. Available from: <https://www.cabidigitallibrary.org/doi/full/10.5555/20103331024>
13. Cao X, Ro KS, Chappell M, Li Y, Mao J. Chemical structures of swine-manure chars produced under different carbonization conditions investigated by advanced solid-state ¹³C nuclear magnetic resonance (NMR). *Environ Sci Technol.* 2011. Available from: <https://doi.org/10.1021/EF101342V>
14. Wang J, Wang Y, Wang J, Du G, Khan KY, Song Y, et al. Comparison of cadmium adsorption by hydrochar and pyrochar derived from Napier grass. *Chemosphere.* 2022;308:136389. Available from: <https://doi.org/10.1016/j.chemosphere.2022.136389>

surface of negatively charged char by electrostatic attraction. In the case of $\text{pH}_{\text{solution}} < \text{pH}_{\text{pzc}}$, high Cd(II) adsorption by PC-CH-300 and PC-CH-500 indicate that electrostatic attraction is an important mechanism during Cd(II) adsorption by biochar [35,36].

In addition, corn husk char had a higher ash content than other char. Alkali and alkaline earth metals such as K, Si, and Mg were detected in EDS analysis. K and Mg contents of PC-CH-300 were 1.74% and 0.23%, respectively. However, these contents were decreased to 0.5% and 0.13%, respectively, after the adsorption experiment. K and Mg contents were 5.11% and 0.57%, respectively, in PC-CH-500. These contents were also decreased to 1.27% and 0.27%, respectively, after the adsorption experiment. Thus, Cd(II) was removed by cation exchange with K, Mg, and so on in PC-CH-300 and PC-CH-500.

Conclusion

This study compared physicochemical properties and Cd(II) adsorption performances of hydrochar and pyrochar generated with cellulose, lignin, and cornhusk as raw materials. It was found that pyrochar produced at the same temperature as hydrochar (300 °C) had a higher char generation yield, ash and oxygen contents, and more developed oxygen functional groups, but lower specific surface area and pore volume than hydrochar. Cd(II) adsorption performances of hydrochar and pyrochar were more suitable with the Langmuir model. When $\text{pH}_{\text{solution}} > \text{pH}_{\text{pzc}}$, surface complexation by oxygen functional groups was observed. When $\text{pH}_{\text{solution}} < \text{pH}_{\text{pzc}}$, electrostatic attraction was found to be an important mechanism of Cd(II) adsorption. Also, when alkali elements such as K and Na were present in biochar, cation exchange was found to be an important mechanism of Cd(II) adsorption removal.

Acknowledgment

This research was supported by the Basic Science Research Program through the National Research Foundation (NRF) funded by the Ministry of Education, Republic of Korea (2022R1A2C1013034).

15. Huff MD, Kumar S, Lee JW. Comparative analysis of pinewood, peanut shell, and bamboo biomass-derived biochars produced via hydrothermal conversion and pyrolysis. *J Environ Manage.* 2014;146:303-308. Available from: <https://doi.org/10.1016/j.jenvman.2014.07.016>
16. Elaigwu SE, Rocher V, Kyriakou G, Greenway GM. Removal of Pb²⁺ and Cd²⁺ from aqueous solution using chars from pyrolysis and microwave-assisted hydrothermal carbonization of *Prosopis Africana* shell. *J Ind Eng Chem.* 2014;20:3467-3473. Available from: <http://dx.doi.org/10.1016/j.jiec.2013.12.036>
17. Babeker TMA, Lv S, Wu J, Zhou J, Chen Q. Insight into Cu(II) adsorption on pyrochar and hydrochar resultant from *Acacia Senegal* waste for wastewater decontamination. *Chemosphere.* 2024;356:141881. Available from: <https://doi.org/10.1016/j.chemosphere.2024.141881>
18. Bonechi C, Consumi M, Donati A, Leone G, Magnani A, Tamasi G, et al. Biomass: An overview. In: *Bioenergy Systems for the Future.* 2017. p. 3-42.
19. Liu Z, Balasubramanian R. Upgrading of waste biomass by hydrothermal carbonization(HTC) and low temperature pyrolysis(LTP): A comparative evaluation. *Appl Energy.* 2014;114:857-864. Available from: <https://ideas.repec.org/a/eee/appene/v114y2014icp857-864.html>
20. Zhang X, Lv L, Qin Y, Xu M, Jia X, Chen Z. Removal of aqueous Cr(VI) by a magnetic biochar derived from *Melia azedarach* wood. *Bioresour Technol.* 2018;256:1-10. Available from: <https://doi.org/10.1016/j.biortech.2018.01.145>
21. Chen Z, Jing Y, Wang Y, Meng X, Zhang C, Chen Z, et al. Enhanced removal of aqueous Cd(II) by a biochar derived from salt-sealing pyrolysis coupled with NaOH treatment. *Appl Surf Sci.* 2020;511:145619. Available from: <https://doi.org/10.1016/j.apsusc.2020.145619>
22. Muley PD, Henkel C, Abdollahi KK, Marculescu C, Boldro D. A critical comparison of pyrolysis of cellulose, lignin, and pine sawdust using an induction heating reactor. *Energy Convers Manag.* 2016;117:273-280. Available from: <https://doi.org/10.1016/j.enconman.2016.03.041>
23. Carpenter D, Westover TL, Czernik S, Jablonski W. Biomass feedstocks for renewable fuel production: A review of the impacts of feedstock and pretreatment on the yield and product distribution of fast pyrolysis bio-oils and vapors. *Green Chem.* 2014;16(2):384-406. Available from: <https://pubs.rsc.org/en/content/articlelanding/2014/gc/c3gc41631c>
24. Van Kreveten DW. Graphical-statistical method for the study of structure and reaction processes of coal. *Fuel.* 1950;29:269-284. Available from: <https://www.scrip.org/reference/referencespapers?referenceid=472246>
25. Chen B, Zhou D, Zhu L. Transitional adsorption and partition of nonpolar and polar aromatic contaminants by biochars of pine needles with different pyrolytic temperatures. *Environ Sci Technol.* 2008;42:5137-5143. Available from: <https://doi.org/10.1021/es8002684>
26. Jaruwat D, Udomsap P, Chollacoop N, Fuji M, Eidad-ua A. Effects of hydrothermal temperature and time of hydrochar from cattail leaves. In: *Int Conf Sci Technol Emerg Mater.* 2010;1:020016. Available from: <http://dx.doi.org/10.1063/1.5053192>
27. Li J, Li Y, Wu Y, Zheng M. A comparison of biochar from lignin, cellulose, and wood as the sorbent to an aromatic pollutant. *J Hazard Mater.* 2014;280:450-457. Available from: <https://doi.org/10.1016/j.jhazmat.2014.08.033>
28. Rutherford DW, Wershaw RL, Cox LG. Changes in composition and porosity occurring during the thermal degradation of wood and wood components. *USGS Scientific Investigations Report* 2004-5292. Available from: <https://doi.org/10.3133/sir20045292>
29. Yan S, Yu W, Yang T, Li Q, Guo J. The adsorption of corn stalk biochar for Pb and Cd: Preparation, characterization, and batch adsorption study. *Separation.* 2022;9(2):22. Available from: <https://doi.org/10.3390/separations9020022>
30. Sangsuk S, Napanya P, Tasen S, Baiya P, Buathong C, Keeratisontornwat K, et al. Production of non-activated biochar based on *Biden pilosa* and its application in removing methylene blue from aqueous solutions. *Cell Press.* 2023;9:e15766. Available from: [https://www.cell.com/heliyon/fulltext/S2405-8440\(23\)02973-0](https://www.cell.com/heliyon/fulltext/S2405-8440(23)02973-0)
31. Zama EF, Zhu YG, Reid BJ, Sun GX. The role of biochar properties in influencing the sorption and desorption of Pb(II), Cd(II), and As(III) in aqueous solution. *J Clean Prod.* 2017;148:127-136. Available from: <http://dx.doi.org/10.1016/j.jclepro.2017.01.125>
32. Gatabi MP, Moghaddam HM, Ghorbani M. Point of zero charge of maghemite decorated multiwalled carbon nanotubes fabricated by chemical precipitation method. *J Mol Liq.* 2016;216:117-125. Available from: <https://doi.org/10.1016/j.molliq.2015.12.087>
33. Tran HN, You SH, Chao HP. Effect of pyrolysis temperatures and times on the adsorption of cadmium onto orange peel derived biochar. *Waste Manag Res.* 2016;34(2):129-138. Available from: <https://doi.org/10.1177/0734242x15615698>
34. Han L, Sun H, Ro KS, Sun K, Libra JA, Xing B. Removal of antimony(III) and cadmium(II) from aqueous solution using animal manure-derived hydrochars and pyrochars. *Bioresour Technol.* 2017;234:77-85. Available from: <https://doi.org/10.1016/j.biortech.2017.02.130>
35. Deng Y, Huang S, Dong C, Meng Z, Wang X. Competitive adsorption behavior and mechanisms of cadmium, nickel, and ammonium from aqueous solution by fresh and aging rice straw biochars. *Bioresour Technol.* 2020;303:122853. Available from: <https://doi.org/10.1016/j.biortech.2020.122853>
36. Jian X, Zhuang X, Li B, Xu X, Wei Z, Song Y, Jiang E. Comparison of characterization and adsorption of biochars produced from hydrothermal carbonization and pyrolysis. *Environ Technol Innov.* 2018;10:27-35. Available from: https://ui.adsabs.harvard.edu/link_gateway/2018EnvTI..10...27J/doi:10.1016/j.eti.2018.01.004

Discover a bigger Impact and Visibility of your article publication with Peertechz Publications

Highlights

- ❖ Signatory publisher of ORCID
- ❖ Signatory Publisher of DORA (San Francisco Declaration on Research Assessment)
- ❖ Articles archived in worlds' renowned service providers such as Portico, CNKI, AGRIS, TDNet, Base (Bielefeld University Library), CrossRef, Scilit, J-Gate etc.
- ❖ Journals indexed in ICMJE, SHERPA/ROMEO, Google Scholar etc.
- ❖ OAI-PMH (Open Archives Initiative Protocol for Metadata Harvesting)
- ❖ Dedicated Editorial Board for every journal
- ❖ Accurate and rapid peer-review process
- ❖ Increased citations of published articles through promotions
- ❖ Reduced timeline for article publication

Submit your articles and experience a new surge in publication services
<https://www.peertechzpublications.org/submission>

Peertechz journals wishes everlasting success in your every endeavours.